



Scholars Research Library

Der Pharma Chemica, 2015, 7(8):217-225
(<http://derpharmachemica.com/archive.html>)



ISSN 0975-413X
CODEN (USA): PCHHAX

Schiff bases of indoline-2,3-dione (isatin) derivatives as efficient agents against resistant strains of *Mycobacterium tuberculosis*[§]

Tarek Aboul-Fadl*, Mohammed K. Abdel-Hamid*[‡] and Adel F. Youssef

Department of Medicinal Chemistry, Faculty of Pharmacy, Assiut University, Assiut, Egypt

[‡]Present address: Centre for Chemical Biology, The University of Newcastle, Callaghan, Australia

[§]This work was presented at the 246th American Chemical Society meeting, Indianapolis, Indiana -USA, September 8-14, 2013

ABSTRACT

A library of 143 Schiff bases of isatin derivatives was evaluated for its activity against the different types of *Mycobacterium tuberculosis*. Ten of the tested derivatives showed promising activity against the wild-type strain with MIC values range between 10-0.156 µg/mL. The most active derivatives (A2, A6, D5 and D8) were further tested against a panel of six single resistant *Mycobacterium tuberculosis* strains. The results revealed interesting results regarding derivative D8 which showed enhanced activity against the Streptomycin resistant strain. Further investigations showed D8 to have equipotent activity to INH against rifampin-resistant strains as well as being 4 times more active than rifampin against the ofloxacin-resistant strains. A pharmacophore modeling study was conducted to determine critical molecular components for activity and to provide insights towards further optimization.

Keywords: Anti-tubercular drugs, Isatin Schiff bases, Pharmacophore

INTRODUCTION

Tuberculosis (TB) is a highly contagious disease caused by *Mycobacterium tuberculosis* (*M. tuberculosis*) and representing the global second leading cause of mortality due communicable diseases [1]. In its "Global Tuberculosis Report 2014", the WHO has estimated about 9 million new TB cases in 2013 leading to more than 1.5 million deaths. Despite such impact on global mortality, the discovery and development of drugs against *M. tuberculosis* have been insufficient to eradicate the disease completely. Moreover, the list for the first line TB chemotherapeutics has remained unchanged in more than five decades. In most affected developing countries, additional factors contribute to the failure of achieving the cure goal. These include inconsistent treatment, patient non-compliance and drugs non-availability. These factors made the development of resistant strains an event that is practically unavoidable [2]. Two categories of drug resistant TB are reported [3]. The first (multidrug resistant, MDR-TB) results from infections by *M. tuberculosis* that are resistant to isoniazid (INH) and rifampin and requires lengthy treatment with the more expensive and toxic second line drug combinations. The second category (extensive drug resistant, XDR-TB) caused by *M. tuberculosis* resistant to INH, rifampin, at least one fluoroquinolone, and one of the injectable drugs such as amikacin [4]. The most recent WHO report shows that 3.5% of new and 20.5% of previously treated TB cases had MDR-TB which means an estimated 480 000 people having developed MDR-TB in 2013 [5]. Moreover, an estimated 9.0% of patients with MDR-TB had XDR-TB. More recently, several reports have warned about the emergence of TB cases that were resistant to all anti-tuberculosis drugs that were tested, a situation that has been termed as 'totally drug resistant' (TDR)-TB [5-7].

Due to the facts mentioned above, new anti-TB drugs and better therapeutic strategies against TB are urgently needed. New drug candidates should shorten the standard treatments and be sufficiently effective against MDR-TB.

Our research group was for many years interested in the developing of new molecules against *M. tuberculosis*[8-12]. In continuation to our synthetic work on Schiff bases of isatin derivatives with potential anti-TB activity[8-12], the current work describes the anti-TB activity of the individual Schiff bases of combinatorial matrix of the isatin derivatives **1-13(A-K)**. Additionally, ligand based pharmacophore modeling of these Schiff bases was conducted to evaluate the common features essential for activity and to predict the hypothetical geometries adopted by these ligands in their most active conformers.

MATERIALS AND METHODS

Chemistry

Isatins and hydrazides building blocks were obtained either commercially or synthesized along with the designed target Schiff bases according to the reported literatures[8-12].

Anti-tubercular and Cytotoxicity Assays

Antitubercular activity of compounds **A-K(1-13)** was investigated at the National Institute of Health and the National Institute of Allergy and Infectious Diseases (NIAID), Bethesda, MD, USA against *M. tuberculosis* H37Rv using Resazurin MIC assay.[14] The single resistant bacteria and H37Rv are grown in Middlebrook 7H9 broth medium (7H9 medium) supplemented with 0.2% (v/v) glycerol, 10% (v/v) ADC (albumin, dextrose, catalase), and 0.05% (v/v) Tween 80. The bacteria were inoculated in 50 ml of 7H9 medium in 1 L roller bottles that are placed on a roller bottle apparatus in an ambient 37 °C incubator. When the cells reach an OD₆₀₀ of 0.150 (equivalent to ~1.5 x 10⁷ CFU/ml), they are diluted 200-fold in 7H9 medium. The assay was conducted using 96-well, U-bottom microplates with an assay volume of 0.2 mL/well. First, the test media, Middlebrook 7H9 broth supplemented with OADC Enrichment (BD BioSciences; Sparks, MD), was added (0.1 mL/well) to each well. The test compounds, solubilized in appropriate solvent and subsequently diluted in test media, were subsequently added (0.1 mL/well) to appropriate wells at twice the intended starting concentration and serially diluted two-fold across the plate. The plates were then inoculated (0.1 mL/well) with a targeted concentration of 1.0 x 10⁶ CFU/mL *M. tuberculosis* and incubated at 37°C for 7 days in approximately 90% humidity. Following incubation, the plates were read visually and individual wells scored for turbidity, partial clearing or complete clearing. Testing was conducted in duplicate and the following controls were included in each test plate: i) medium only (sterility control); ii) organism in medium (negative control); and iii) rifampin or isoniazid (positive control). The MIC is reported as the lowest concentration (µg/mL) of drug that visually inhibits growth of the organism. Minimal Bactericidal Concentration (MBC) is determined subsequent to MIC testing by sub-culturing diluted aliquots from wells that fail to exhibit macroscopic growth. The sample aliquots are inoculated onto Middlebrook 7H10 agar plates and then incubated for 16-21 days at 37 °C. Once growth is apparent, the bacterial colonies are enumerated. The MBC is defined as the lowest concentration (µg/mL) of compound exhibiting 99.9% kill over the same time period used to determine the MIC (18-24 h). MBC values greater than 16 times the MIC typically indicate antimicrobial tolerance.

Cytotoxicity was done at Stem Cell Therapy Program, King Faisal Specialized Hospital and Research Center, Riyadh-Saudi Arabia according to the previously reported protocol.[13]

Pharmacophore modelling

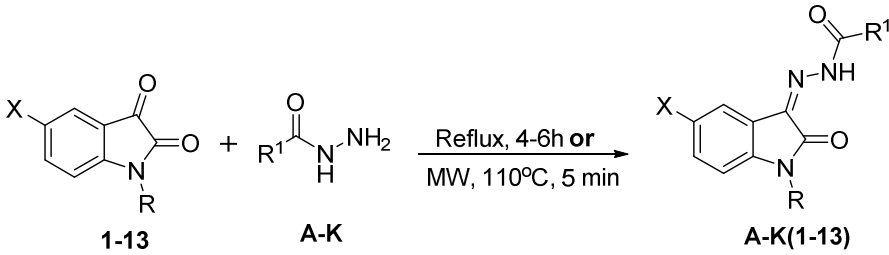
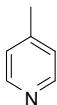
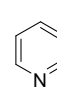
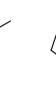
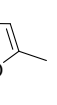
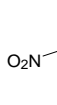
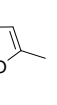
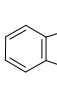
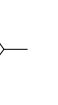
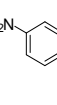
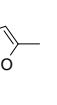
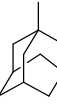
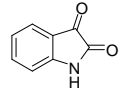
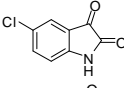
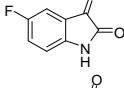
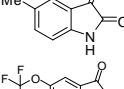
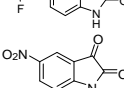
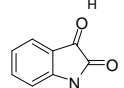
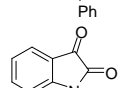
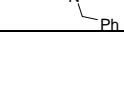
Pharmacophore hypotheses were generated using of Accelrys Discovery Studio 2.5 (DS) software (Accelrys, Inc., San Diego, CA 92121, USA). Molecules were edited using the DS 3D visualizer while conformational models for each compound were generated using the Poling Algorithm. The “best conformational search” option was used, specifying 250 as the maximum number of conformers. The models emphasized a conformational diversity under the constraint of 20 kcal/mol energy threshold above the estimated global minimum based on use of the CHARMM force field. The molecules associated with their conformational models were submitted to HipHop hypothesis generation. The features selected for this run were hydrogen bond donor (HBD), hydrogen bond acceptor (HBA), positive ionizable (PI), negative ionizable (NI), hydrophobic (HY) and aromatic (R) features.

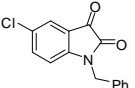
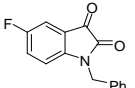
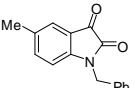
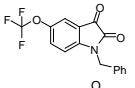
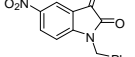
RESULTS AND DISCUSSION

Activity and selectivity against wild-type *M. tuberculosis*

The majority of the individual 14 Schiff base compounds **A-K(1-13)** were already reported and the synthesis of the novel derivatives has relied on our established synthetic protocol (Table 1)[10, 11, 13]. Briefly, the reaction was carried out starting from a suitable isatin building block and the corresponding hydrazide derivative. Both starting materials were dissolved in ethanol under acidic conditions and the obtained solution was subjected to either conventional or microwave heating [10, 11]. The obtained products were purified by recrystallization from suitable solvent and their structures were confirmed through spectral analyses.

Table 1. Schiff bases of indoline-2,3-dione (isatin) derivatives used in this study

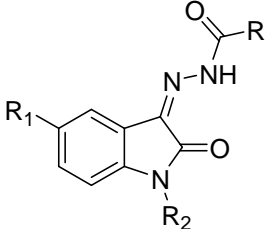
												
		A	B	C	D	E	F	G	H	I	J	K
												
1		A1	B1	C1	D1	E1	F1	G1	H1	I1	J1	K1
2		A2	B2	C2	D2	E2	F2	G2	H2	I2	G2	K2
3		A3	B3	C3	D3	E3	F3	G3	H3	I3	G3	K3
4		A4	B4	C4	D4	E4	F4	G4	H4	I4	G4	K4
5		A5	B5	C5	D5	E5	F5	G5	H5	I5	G5	K5
6		A6	B6	C6	D6	E6	F6	G6	H6	I6	G6	K6
7		A7	B7	C7	D7	E7	F7	G7	H7	I7	G7	K7
8		A8	B8	C8	D8	E8	F8	G8	H8	I8	G8	K8

9		A9	B9	C9	D9	E9	F9	G9	H9	I9	G9	K9
10		A10	B10	C10	D10	E10	F10	G10	H10	I10	G10	K10
11		A11	B11	C11	D11	E11	F11	G11	H11	I11	G11	K11
12		A12	B12	C12	D12	E12	F12	G12	H12	I12	G12	K12
13		A13	B13	C13	D13	E13	F13	G13	H13	I13	G13	K13

The anti-TB activity of the reported derivatives was evaluated against *M. tuberculosis* H37Rv at the National Institutes of Health (NIH) and the National Institute of Allergy and Infectious Diseases (NIAID), Bethesda, MD, USA. Compounds were initially tested at a single point concentration of 10 µg/ml. Derivatives that show significant activity at this initial screening were then further tested in an MIC assay at 8 concentrations ranging between 10 and 0.078 µg/ml using INHand rifampin as reference drugs. Unfortunately, due to the limited solubility of most isatin based compounds under the assay conditions, only biological data for derivatives **A2**, **A3**, **A6**, **D3**, **D5**, **D7-D11** were obtained (Table 2).

The data shows moderate anti-TB activity for compounds from the **A** and **D** series with **D8** and **D10** being the most active derivatives (0.156 µg/mL). It is not clear at this point whether the carbonyl carrier, **1-13**, or the hydrazine carrier, **A-K**, moieties maintained the upper hand in anti-TB activity. However, preliminary SAR data shows preferences for nicotinic acid and 5-nitro-furanyl moieties. Comparing the active derivatives of series **A** (**A2**, **A3** and **A6**) with their analogues in series **B** revealed that the point of pyridyl point attachment is critical for activity. Substitution at the isatin nitrogen doesn't favor activity for series **A** while it was found to greatly enhance the activity of series **D**. Interestingly, the substitution pattern showed in series **D** is consistent with our previous observation and the design hypothesis of these molecules [8]. We believe that it is the integrated molecular structure features that are responsible for the elucidated activity irrespective of the building blocks corporate in individual molecules. We hope that solving the solubility problems for the synthesized molecules would shed more light on the SAR of these type of anti-TB agents.

Table 2: *In vitro* Antitubercular activity against *Mycobacterium tuberculosis* H37Rv, Cytotoxicity against MCF-12A cell line and selectivity Index (□M) of the active synthesized Schiff bases



Compd	Structure			MIC (µg/ml)	Cytotoxicity (IC ₅₀ /□Mol)	Selectivity Index (IC ₅₀ /MIC)
	R	R ₁	R ₂			
A2		Cl	H	1.25	47.33	11.38
A3		F	H	10	16.48	2.13
A6		NO ₂	H	0.312	88.15	88.15
D3		F	H	5	129.76	8.26
D5		OCF ₃	H	2.5	7.51	1.15
D7		H	Ph	5	15.49	1.17
D8		H	PhCH ₂	0.156	18.23	45.58
D9		Cl	PhCH ₂	0.312	11.26	15.42
D10		F	PhCH ₂	0.156	38.94	102.47
D11		CH ₃	PhCH ₂	1.25	- ^a	
Rifampin		NT		0.0031	NT ^b	NT
Isoniazid		NT		0.063	NT	NT

^a Inactive up to 200µM range.

^b Not tested.

Compounds which showed significant anti-TB activity (**A2**, **A6**, **D2**, **D5**, **D7-11**) were also examined for their cytotoxicity (IC₅₀) in normal MCF-12A cell line. Most of the tested compounds show low toxicity with generally high selectivity (1.15 to more than 102.47µM) towards the TB cells. It is noteworthy that the Schiff bases carrying the 5-nitrofuryl moiety revealed the most active (**D8-D10**) as well as the most selective (**D10**).

Activity against single mutant *M. tuberculosis* strains

Compounds **A2**, **A6**, **D5** and **D8** were selected to be tested against a panel of six single resistant strains of *Mycobacterium tuberculosis* and to calculate their minimum bacteriostatic activity (MBC) against the wild-type strain (Table 3).

The data showed that MBC values of the 4 compounds obtained with H37Rv were similar to their MIC values. The results revealed comparable activities for the tested compounds against the used resistant strains. Surprisingly, compound **D8** showed an order of magnitude enhancement in its activity against the streptomycin-resistant strain. This result encouraged us to further test **D8** against rifampin- and ofloxacin-resistant strains. In an agreement with its inhibition for the streptomycin-resistant strains, the derivative **D8** showed high inhibition against rifampin- and as well as ofloxacin-resistant strains (0.024 and 0.098µg/ml respectively). Also, the obtained results found **D8** to

show equipotent activity to INH against rifampin-resistant strains and to be 4 times more active than rifampin against the ofloxacin-resistant strains. These exciting findings puts the isatin Schiff base derivative **D8** as a potential lead compound for further developing of this type of compounds against resistant *M. tuberculosis* strains.

Table 3 : *In vitro* Antitubercular activity of selected derivatives against a panel of single resistant *Mycobacterium tuberculosis*

Compd	ATCC 35820 ^a	ATCC 35821 ^b	ATCC 35822 ^c	ATCC 35827 ^d	ATCC 35830 ^e	ATCC 35837 ^f	OFX-R ^g	RMP-R ^h	MBC ⁱ (µg/ml)
A2	1.25	1.25	>10	1.25	10	1.25	- ^j	-	1.25
A6	0.156	0.156	>10	0.312	2.5	0.156	-	-	0.31
D5	1.25	2.5	5	5	2.5	2.5	-	-	2.5
D8	<0.078	0.312	0.156	0.156	0.156	0.156	0.098	0.024	0.156
RIF	-	-	-	-	-	-	0.390	-	-
INH	-	-	-	-	-	-	-	0.02	-

^a Streptomycin-resistant, ^b p-aminosalicylic acid-resistant, ^c Isoniazid-resistant, ^d Kanamycin-resistant, ^e Ethionamide-resistant, ^f Ethambutol-resistant, ^g Ofloxacin-resistant, ^h Rifampin-resistant, ⁱ Performed with H37Rv, ^j Not tested.

Pharmacophore modelling

Initial model generation

Derived by the promising activity of the tested compounds, a 3D pharmacophore model based on the active molecules was generated. The model aims to identify the molecular components that are critical for activity as well as provide necessary information for further optimization. Derivatives which showed significant anti-TB activity (**A2**, **A6**, **D3**, **D5**, **D7-D11**) were considered as the training set for the pharmacophore generation using HipHop module of the Accelrys Discovery Studio modeling engine. For the optimized run the highest weight was assigned to the most active compounds (**A6**, **D8-D10**). The HipHop run resulted in the generation of 10 hypotheses (Hypo1-Hypo10), each of them is composed of four features (Table 4). The first five hypotheses (Hypo1-Hypo5) are composed of the same molecular features and are showing close ranking scores. Interestingly, all hypotheses have shown complete mapping of their features to the training set compounds (direct hit).

Table 4: Summary of HipHop generated common feature hypotheses

Hypothesis	Features ^a	Rank score	Direct hit ^b	Partial hit ^c
1	RAAA	92.767	11111111	00000000
2	RAAA	92.698	11111111	00000000
3	RAAA	91.151	11111111	00000000
4	RAAA	90.161	11111111	00000000
5	RAAA	90.161	11111111	00000000
6	HHHA	89.915	11111111	00000000
7	RAAA	89.617	11111111	00000000
8	HHHA	89.181	11111111	00000000
9	RAAA	88.820	11111111	00000000
10	RAAA	88.813	11111111	00000000

^aR, ring aromatic; H, hydrophobic; A, hydrogen bond acceptor.

^b Direct hit indicates whether (1) or not (0) a molecule in the training set mapped to every feature in the hypothesis.

^c Partial hit indicates whether (1) or not (0) a molecule in the training set mapped to all but one feature in the hypothesis.

Optimization of highest ranked hypotheses

The identical structural features and the close rank scores shown by Hypo1-Hypo5 required further investigation to assign the difference between their features. Calculating the distance matrix (DM) between the generated pharmacophores Hypo1-Hypo5 (SI, Table S1) showed a close correlation between hypotheses with a maximum distance of 0.077. This close relation was encouraging for the construction of a median pharmacophore. This pharmacophore (model 1) was based on the same structural features for Hypo1-Hypo5 while positioning each feature coordinates to a median position in relation to its location within the five hypotheses. Model 1 (**Fig. 1**) shows a five featured pharmacophore composed of ring aromatic (RA) and three hydrogen bond acceptor (HBA_1-HBA_3) features. The RA feature was found to be terminal and well distanced from the central HBA_1 and HBA_3. On the other hand, HBA_2 lays on the reverse pole 10.0 and 6.2 Å far from the central features.

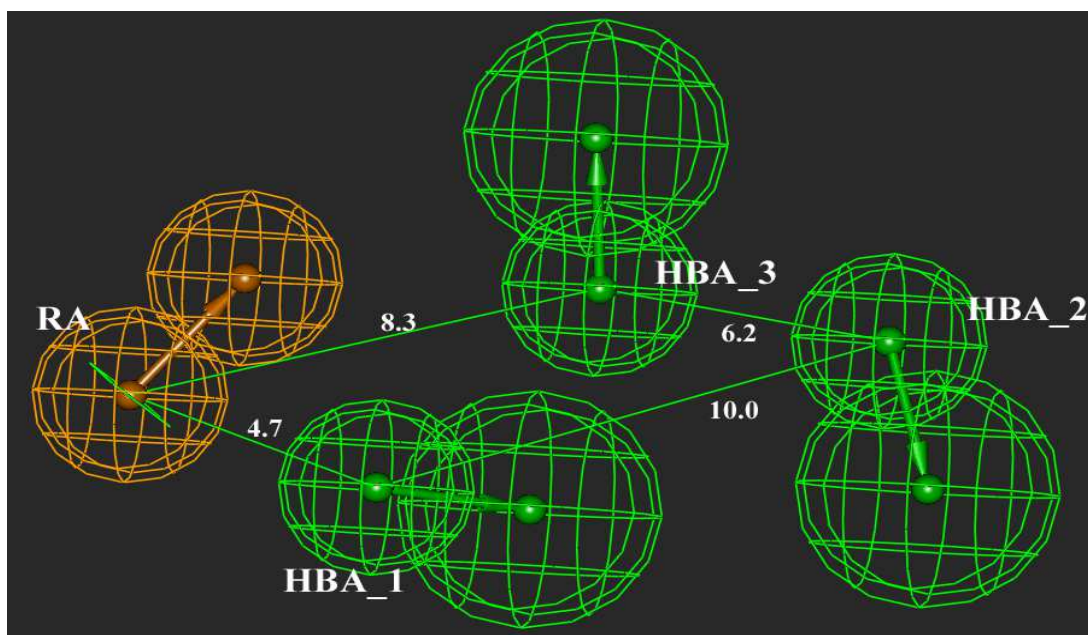


Figure. 1: Model 1 pharmacophore hypothesis showing intra feature distances (Å). Features are colour coded as: Hydrogen bond acceptor (HBA), green; ring aromatic (RA), brown

Model refinement by addition of “excluded volumes” constrains

Despite the suggestion that the inactivity of most of the synthesized compounds is, at least partially, due to their poor solubility in the assay medium, a list of the inactive molecules were used for model 1 refinement. This molecular list was carefully chosen to include 12 molecules covering the different structural categories of the tested compounds (L2, M5, N3, O2, P2, E4, F3, G5, H2, I7, J8 and K6). The purpose of this refinement is to produce a model which is more restrict and able to discriminate inactive molecules. The refinement results in the generation of two sets of “excluded volumes” that were added to model 1 affording a new and more restrict hypothesis (model 2). The added excluded volume features were placed proximal to the terminal features RA and HBA_2 (Fig. 2). These excluded volumes represent areas of restrictions to the presence of any molecular fragments and was decided based on the set of the inactive compounds.

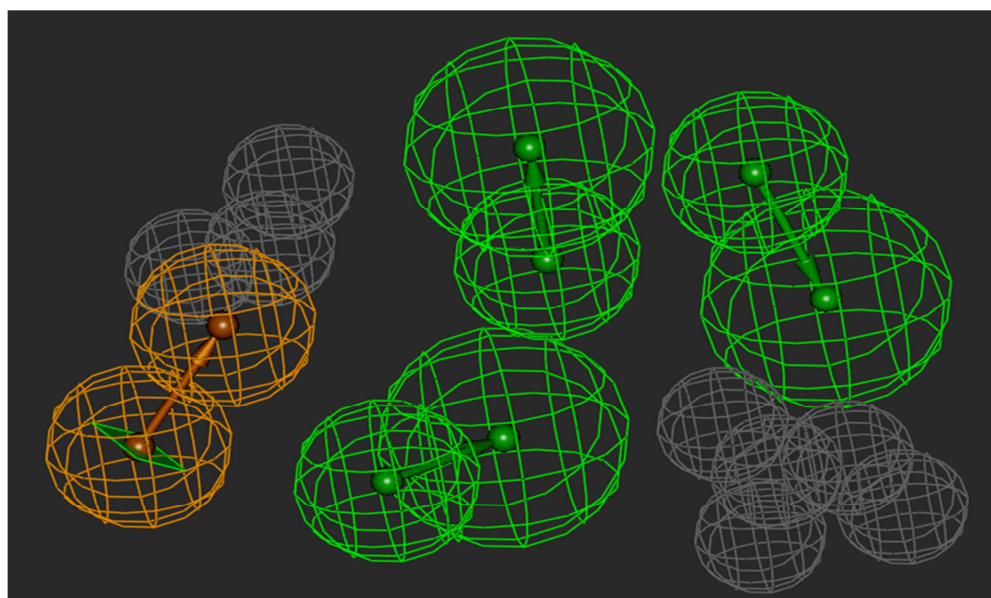


Figure 2: Model 2 showing the refinement of the hypothesis by the placement of excluded volume features (grey)

At this stage, model 2 was tested for its ability to predict the activity of tested compounds. The training set compounds was mapped into model 2 using the “best fit” option in DS software. HipHop scores the orientation of a mapped compound within the hypothesis features using a “fit value” score. The mapping results (Table 5) show fitting of most of the tested compounds into the pharmacophoric features with fit values ranges from 1.7 to 4.0. A

moderate correlation between the fit values of the mapped compounds and their biological activities was observed. As a general observation, compounds that carry a furan side chain (**D3**, **D5**, **D7-D11**) have shown better fit value to model 2. Closer inspection of the fit values of these compounds shows an excellent correlation between the IC_{50} and the fit values with R^2 value of 0.933 and a standard error (SE) as low as 0.232. Unfortunately, adding the derivatives A2 and A6 to the regression results in a dramatic decrease in the R^2 to a value of 0.561 with SE value of 0.630.

Table 5: Output for mapping the tested compounds into “model 2”

Compound	IC_{50} (μ M)	Fit value	E (kcal/mol) ^a
A2	1.25	1.7	7.41
A6	0.321	2.8	5.36
D3	5	1.9	0.97
D5	2.5	2.6	0.59
D7	5	2.3	1.31
D8	0.156	4.0	12.66
D9	0.321	3.8	5.93
D10	0.156	3.7	10.42
D11	1.25	3.3	8.6

^a Energy of the fitted conformer relative to its global minimum energy

Analysis of the mapped structures into “model 2”

Inspection of the superimposed mapping of the training set compounds into model 2 highlights key structural features for activity (SI, Fig. S1). The nitrofuran group found to play an important role for fitting into the HBA_2 feature where the nitro group plays as the hydrogen bond accepting center. In case of compounds A2 and A6, this feature was accommodated by the nitrogen atom of the pyridine ring. However, the center of the hydrogen acceptor vector doesn't overlay well onto the pyridine nitrogen for both molecules. This may explain the limitation of the model to accurately predict the activities for A2 and A6. Further study based on the addition of derivatives with variable hydrogen bond acceptor groups at this position may be necessary in order to optimize the 3D placement of this feature.

Interestingly, the restrict position of this hydrogen bond acceptor feature explains the complete inactivity of compounds from series **B** despite being structurally very close to the **A** series compounds. **Fig. 3** shows that while **A2** can map its pyridine nitrogen partially into HBA_2, the shift of the nitrogen to the ring position 3 led to failure of **B2** to map into the same feature similarly.

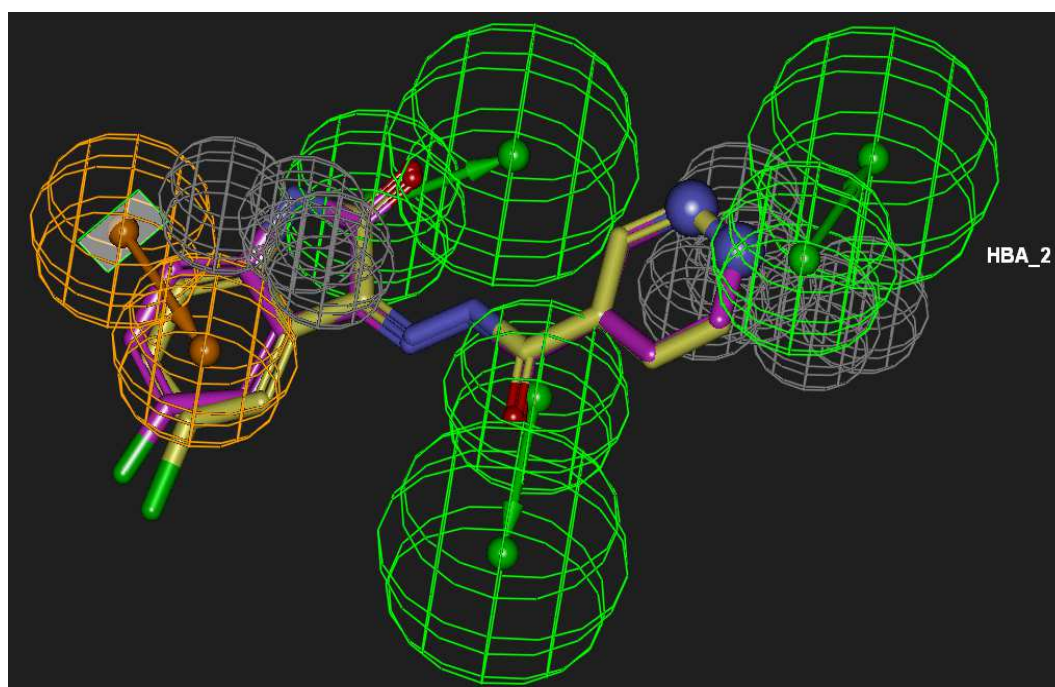


Figure3: Superimposed mapping of A2 (carbon atoms in pink) and B2 (carbon atoms in yellow) into model 2

The fourth pharmacophoric feature in model 2 is the ring aromatic (RA) feature. This feature was best filled with the *N*-benzyl substituent of derivatives D8-D11. These derivatives found to orient the terminal phenyl ring perfectly into the RA feature (**Fig. 4**). However, the absence of this benzyl moiety in other derivatives doesn't prevent the

occupancy of the RA feature. In this case, the RA feature was mapped through shifting the orientation of the indoline moiety so that its benzo part can be placed within the RA feature space (SI, Fig. S2).

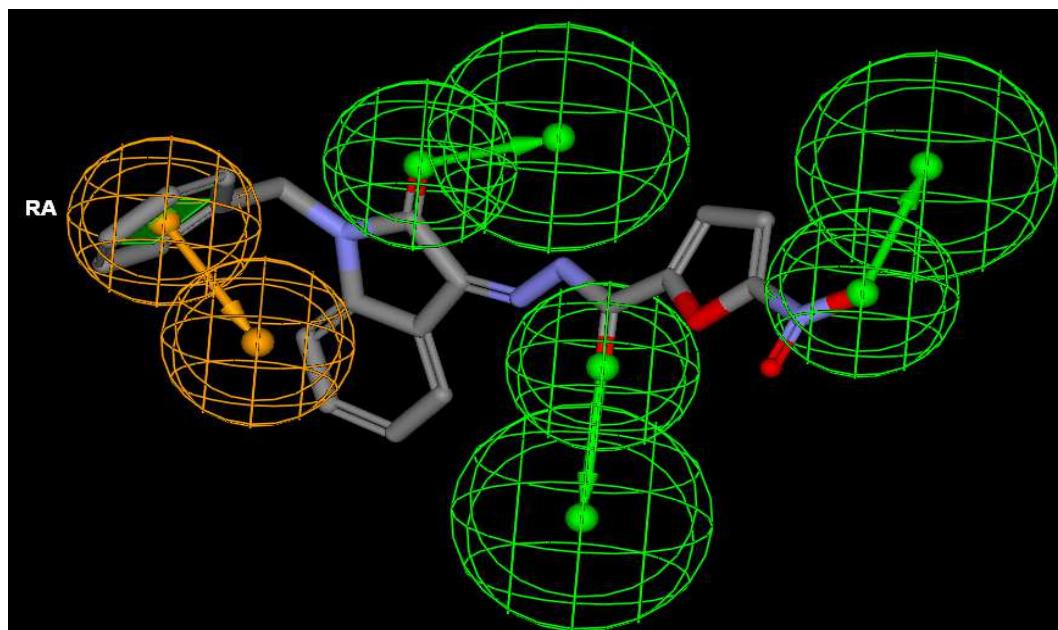


Figure4: Mapping of D8 into model 2 pharmacophore showing the orientation of the N-benzyl side chain into the RA feature (excluded volumes feature is hidden for simplicity)

Finally, the inclusion of the “excluded volumes” feature was helpful to define larger molecules as inactive entries. Derivatives of group E-K were unable to fit into the model. The bulky side chain, that replaces either the furan or the pyridine ring in the active molecules, was found to have a steric clash with “excluded volume” features.

CONCLUSION

Based on a library of 143 Schiff base derivatives of isatin we have successfully identified ten compounds as potential anti-tubercular candidates. The tested compounds have shown low normal cell toxicity with significant selectivity against the bacterial cells. Further investigations including a panel of six single resistant *M. tuberculosis* mutants have introduced **D8** as an attractive anti-tubercular agent. Results showed **D8** to possess an equipotent activity to INH against rifampin-resistant *M. tuberculosis* strains and 4 times higher activity than rifampin- against the ofloxacin-resistant strains. Pharamcophore modelling study was conducted using a selected set of the tested compounds to evaluate structural components necessary for the apparent activity. The exciting results reported here puts the isatin Schiff base derivative **D8** as a potential lead compound for further developing against resistant *M. tuberculosis* strains.

REFERENCES

- [1] M Raviglione, Uplekar M, Vincent C, Pablos-Méndez A. *The Lancet Global Health*. 2, e71-e2.
- [2] T Tanimura, Jaramillo E, Weil D, Raviglione M, Lönnroth K. *Eur Respir J*. **2014**, 43, 1763-75.
- [3] E Pontali, Matteelli A, Migliori GB. *Curr Opin Pulm Med*. **2013**, 19, 266-72.
- [4] Daniel E Goldberg, Siliciano Robert F, Jacobs Jr William R. *Cell*. **2012**, 148, 1271-83.
- [5] GB Migliori, Sotgiu G, Gandhi NR, Falzon D, DeRiemer K, Centis R, et al. *Eur Respir J*. **2013**, 42, 169-79.
- [6] ZF Udhwadia, Amale RA, Ajbani KK, Rodrigues C. *Clin Infect Dis*. **2012**, 54, 579-81.
- [7] AA Velayati, Masjedi MR, Farnia P, Tabarsi P, Ghanavi J, ZiaZarifi AH, et al. *Chest*. **2009**, 136, 420-5.
- [8] WS Abdel-Aal, Hassan HY, Aboul-Fadl T, Youssef AF. *Eur J Med Chem*. **2010**, 45, 1098-106.
- [9] T Aboul-Fadl, Bin-Jubair FAS, Aboul-Wafa O. *Eur J Med Chem*. **2010**, 45, 4578-86.
- [10] T Aboul-Fadl, Abdel-Aziz HA, Kadi A, Ahmad P, Elsaman T, Attwa MW, et al. *Molecules*. **2011**, 16, 5194.
- [11] T Aboul-Fadl, Abdel-Aziz HA, Abdel-Hamid MK, Elsaman T, Thanassi J, Pucci MJ. *Molecules*. **2011**, 16, 7864.
- [12] T Aboul-Fadl, Mohammed F-H, Hassan E-S. *Arch Pharm Res*. **2003**, 26, 778-84.
- [13] T Aboul-Fadl, Radwan AA, Attia MI, Al-Dhfyan A, Abdel-Aziz HA. *Chemistry Central Journal*. **2012**, 6, 49-.
- [14] L Collins, Franzblau SG. *Antimicrob Agents Chemother*. **1997**, 41, 1004-9.